

## Effects of pressure and distortion on superconductivity in $Tl_2Ba_2CaCu_2O_{8+}$

This content has been downloaded from IOPscience. Please scroll down to see the full text.

2015 J. Phys.: Condens. Matter 27 445701

(<http://iopscience.iop.org/0953-8984/27/44/445701>)

View [the table of contents for this issue](#), or go to the [journal homepage](#) for more

Download details:

IP Address: 38.127.180.2

This content was downloaded on 13/10/2015 at 10:44

Please note that [terms and conditions apply](#).

# Effects of pressure and distortion on superconductivity in $Tl_2Ba_2CaCu_2O_{8+\delta}$

HPSTAR  
0122—2015Jian-Bo Zhang<sup>1,2,3</sup>, Viktor V Struzhkin<sup>3,2</sup>, Wenge Yang<sup>2,3</sup>, Ho-Kwang Mao<sup>2,3</sup>,  
Hai-Qing Lin<sup>4</sup>, Yong-Chang Ma<sup>5</sup>, Nan-Lin Wang<sup>6,7</sup> and Xiao-Jia Chen<sup>2,3</sup><sup>1</sup> Department of Physics, South China University of Technology, Guangzhou 510640, People's Republic of China<sup>2</sup> Center for High Pressure Science and Technology Advanced Research, Shanghai 201203, People's Republic of China<sup>3</sup> Geophysical Laboratory, Carnegie Institution of Washington, Washington, DC 20015, USA<sup>4</sup> Beijing Computational Science Research Center, Beijing 100089, People's Republic of China<sup>5</sup> School of Materials Science and Engineering, Tianjin University of Technology, Tianjin 300384, People's Republic of China<sup>6</sup> International Center for Quantum Materials, School of Physics, Peking University, Beijing 100871, People's Republic of China<sup>7</sup> Collaborative Innovation Center of Quantum Matter, Beijing 100871, People's Republic of ChinaE-mail: [xjchen@hpstar.ac.cn](mailto:xjchen@hpstar.ac.cn)

Received 21 July 2015, revised 18 September 2015

Accepted for publication 22 September 2015

Published 13 October 2015



CrossMark

## Abstract

The systematic evolution of the structural, vibrational, and superconducting properties of nearly optimally doped  $Tl_2Ba_2CaCu_2O_{8+\delta}$  with pressure up to 30 GPa is studied by x-ray diffraction, Raman scattering, and magnetic susceptibility measurements. No phase transformation is observed in the studied pressure regime. The obtained lattice parameters and unit-cell volume continuously decrease with pressure by following the expected equation of state. The axial ratio of  $c/a$  exhibits an anomaly starting from 9 GPa. At such a pressure level, the deviation from the nonlinear variation of the phonon frequencies is detected. Both the above observations indicate the enhancement of the distortion upon compression. The superconducting transition temperature is found to exhibit a parabolic behavior with a maximum of 114 K around 7 GPa. We demonstrate that the interplay between the intrinsic pressure variables and distortion controls the superconductivity.

Keywords: pressure, superconductivity, distortion, Raman, x-ray diffraction

(Some figures may appear in colour only in the online journal)

## 1. Introduction

Superconductivity in cuprates usually appears at certain doping levels in which spin and charge stripes [1], pseudogap [2–4], spin glass [5], charge order [6–8], antiferromagnetic [9] and charge density wave [10] coexist and/or compete with superconductivity. Whether a general principle underlies the relationship between superconductivity and these competing orders is an outstanding question. Finding its answer(s) would eventually revolutionize condensed matter physics. Even an empirical connection between superconductivity and competing orders could offer new opportunities to the search for novel superconducting materials.

Lattice distortion has been generally observed to significantly affect the superconducting transition temperature  $T_c$  of many cuprates [11–19]. Distortion is usually introduced into the cation sites in the plane adjacent to the  $CuO_2$  plane through the cation substitution [13–19]. In the  $La_2CuO_4$ -based system, fixing the mean A-site cation radius of the optimally doped compounds, the only change of the size variance also can rapidly suppress  $T_c$  in the same manner as the substitution of diamagnetic elements such as Zn for Cu [11, 12]. The single-layer  $Bi_2Sr_2CuO_{6+\delta}$  was suggested to share the similar mechanism for the distortion effect on superconductivity [15]. However, a systematic study [16] on both  $Bi_2Sr_2CuO_{6+\delta}$

and  $\text{Bi}_2\text{Sr}_2\text{CaCu}_2\text{O}_{8+\delta}$  revealed that the cation distortion is in reality associated with the chemical inhomogeneities. The superconducting gap of the latter was reported to be suppressed with increasing distortion mainly in the nodal region while the antinodal gap remains almost unchanged [17]. Phase separation was also proposed to accompany with lattice distortion in  $\text{YBa}_2\text{Cu}_3\text{O}_{7-\delta}$  (Y123)-based materials when tuning their superconductivity through cation substitution [18, 19]. The accompaniment of chemical inhomogeneities or phase separation to distortion [16, 18, 19] adds the complexity in the analysis of its effects on superconductivity. Therefore, the impact of distortion on the electronic structure and superconducting properties in high- $T_c$  cuprates is still not clear, a task which is very difficult even in conventional superconductors [20]. Searching for a cleaner variable to tune and control superconductivity at fixed doping level is emergent and attractive.

Pressure changes a material only through lattice compression without bringing about any impurities and thus it has been recognized as one clean variable for satisfying these demands. The developments of high-pressure techniques in the past half a century has already enabled the measurements at ambient conditions available at high pressures. In fact, superconductivity studies [21–24] benefited a lot from these technique developments. The record high  $T_c$  of 164 K in cuprates [25] and the new record for superconductivity at 203 K in H-S system [26] were achieved at high pressures. Interestingly, Calamitou *et al* [27, 28] emphasized the distortion effects and phase separation on superconductivity under pressure in two superconductors  $\text{YBa}_2\text{Cu}_4\text{O}_8$  (Y124) and Y123 and non-superconducting  $\text{PrBa}_2\text{Cu}_3\text{O}_{6.92}$  by combining synchrotron x-ray diffraction (XRD) and Raman spectroscopy measurements. Their analysis strongly shows a clear anomaly in the evolutions of both the lattice parameters and phonon modes with pressure in these systems. The distortion was observed to start increasing with pressure when the anomaly appears. The observed phase separation is analogous to the one previously reported by the same authors in these systems at ambient pressure [18, 19]. Recently, Nakayama *et al* [29] investigated the crystal structure and electrical resistivity of Y124 under pressure up to 18 GPa. A dramatic change of  $T_c$  was observed to be accompanied by a structural phase transition around 10 GPa. This study is followed by Raman spectroscopy and *ab initio* calculations [30], which confirm the phase transition. Such complexities call for a careful examination of the roles of pressure, distortion, and phase separation/transition on superconductivity by combing multiple techniques based on the same sample.

Lattice instability and structural fluctuation have been generally observed in thallium-based cuprate superconductors [10, 31–35] through the measurements of electron-diffraction, far-infrared reflectivity, and Cu K-edge extended x-ray-absorption fine structure, suggesting a close connection between lattice degrees of freedom and superconductivity. This superconducting family thus offers a good opportunity to examine the lattice distortion effects on superconductivity.

In this work, we choose a well characterized bilayer  $\text{Tl}_2\text{Ba}_2\text{CaCu}_2\text{O}_{8+\delta}$  (Tl2212) single crystal and investigate the pressure effects on lattice evolution, vibrational properties,

and superconductivity to address the above mentioned issues. Our central experimental finding is that the distortion of this superconductor develop with pressure above 10 GPa, and  $T_c$  undertakes a significant change over the pressure range studied. Our results indicate that the pressure dependence on superconductivity is controlled by both the intrinsic parameters themselves and the distortion in the studied system.

## 2. Experimental details

The nearly optimally doped Tl2212 single crystal with  $T_c$  of 109 K was grown by the flux method [36]. For getting good powder diffraction data, one piece of single crystal was crashed and grounded carefully to make fine powder grains without large strain. A small piece of sample pellet together with a small ruby ball was loaded to a symmetric diamond anvil cell (DAC) with culet of 300  $\mu\text{m}$  for the powder XRD measurement under pressure. The sample chamber of about 110  $\mu\text{m}$  in diameter was created in a gasket made by the stainless steel. Neon gas was loaded into the sample chamber as the pressure medium using the GSECARS gas loading system at the Advanced Photon Source, Argonne National Laboratory [37].

XRD patterns were collected by a MAR345 image plate at pressures up to 25.6 GPa at room temperature, by using Beamline at 16BM-D of High Pressure Collaborative Access Team at the Advanced Photon Source, with an incident x-ray wavelength of 0.509 17 Å. The two dimensional patterns were integrated into one dimensional XRD patterns with Fit2D software [38]. The intensity-versus- $2\theta$  diffraction patterns were analyzed in terms of the Le Bail method by using GSAS software [39, 40].

High-pressure Raman measurements were carried out by using a DAC for ZZ polarization. The single crystal sample with size of  $50 \times 50 \times 20 \mu\text{m}^3$  was loaded into the sample chamber being about 130  $\mu\text{m}$  in diameter and 35  $\mu\text{m}$  in thickness. Daphne 7373 was loaded inside as the pressure transmitting medium. The 532 nm line from an Nd-YAG laser was used for excitation with power less than 10 mW.

We adopted a highly sensitive magnetic susceptibility technique developed for DAC to determine  $T_c$  at high pressures, as described before [21–24]. The technique is based on the quenching of the superconductivity and suppression of the Meissner effect in the superconducting sample by an external magnetic field. The magnetic field applied to the sample inserted in the DAC mainly affects the change of the signal coming from the sample. The  $T_c$  is then identified as the point where the signal goes to zero because of the disappearance of the Meissner effect. An ac circuit includes a signal coil, a compensating coil, a high-frequency excitation coil and a low-frequency modulating coil. A single crystal with dimensions of  $120 \times 100 \times 20 \mu\text{m}^3$  was loaded into a Mao-Bell DAC which was made from hardened Be-Cu alloy. A nonmagnetic Ni-Cr alloy gasket was preindented to 35  $\mu\text{m}$  thick with a hole of 250  $\mu\text{m}$  in diameter to serve as the sample chamber. For direct comparison, we chose Daphne 7373 as the same pressure transmitting medium as for the Raman measurements.

For all these measurements, pressure was gauged by the shift of the R1 fluorescence line of ruby [41].

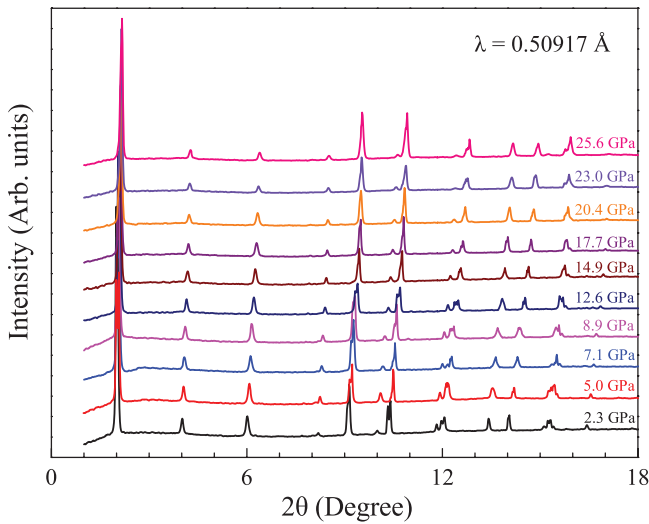


**Figure 1.** The integrated powder x-ray diffraction data of the nearly optimally doped  $\text{Tl}_2\text{Ba}_2\text{CaCu}_2\text{O}_{8+\delta}$  at various pressures up to 25.6 GPa.

### 3. Results and discussion

#### 3.1. X-ray diffraction

The XRD patterns for the nearly optimally doped Tl2212 are shown in figure 1 at various pressures and room temperature. All diffraction peaks monotonically shift to higher angles with increasing pressure. There are no new diffraction peaks and no peak merging and/or splitting. These behaviors indicate that the structure of Tl2212 was stable under pressure. This result is different to the pressure-induced phase separation observed in Y123 superconductor [28], in which new diffraction peaks appear at pressure around 3.7 GPa and lattice parameters show abnormal behaviors at pressure range of 3.7 and 10 GPa. Our diffraction data does not support pressure-induced phase transition or phase separation in Tl2212.

Tl2212 has a tetragonal unit cell with a space group of  $I4/mmm$  determined from the single crystal XRD and neutron powder diffraction measurements [42, 43]. The unit cell consists of two insulating Tl–O and Ba–O blocking layers and two structurally equivalent Cu–O plans separated by Ca layer. Figure 2 illustrates the powder XRD data and a typical Le Bail fitting of the nearly optimally doped Tl2212 at pressure of 2.3 GPa based on this structure model. The fitting yields reasonable factors of  $R_p = 1.4\%$ ,  $R_{wp} = 2.8\%$ , and  $\chi^2 = 4.8\%$ . All patterns were fitted well with  $I4/mmm$  up to 25.6 GPa. These results indicate that Tl2212 remains in the tetragonal structure at the pressure regime studied.

The evolution of distortion with pressure was usually studied by combining XRD and Raman measurements [27, 28]. The change in distortion with pressure can be judged by two basic facts: (i) Pressure-induced lattice anomalies (the lattice parameters and cell volume exhibit obvious deviations from the expected equation of state); (ii) The unconventional variation of both the phonon frequencies and widths of some modes with increasing pressure. The existence of the distortion in the thallium-based cuprates at ambient pressure has been reported

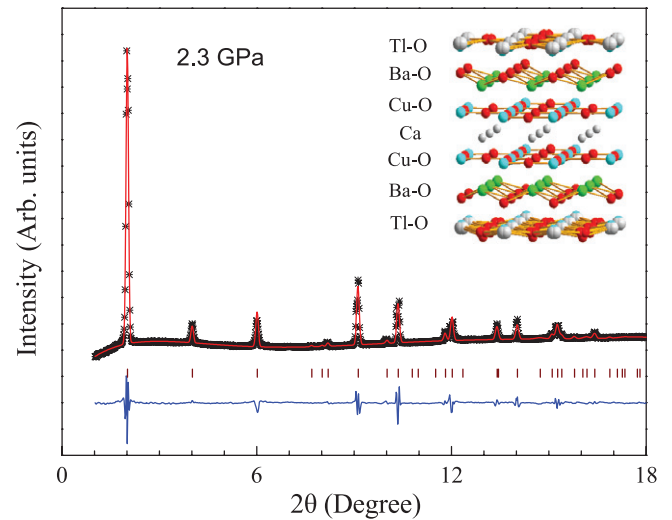


**Figure 2.** The observed x-ray diffraction pattern (stars), Le Bail fit (upper continuous red line), and difference between the observed and calculated profiles (bottom blue line) obtained after Le Bail fitting of the nearly optimally doped  $\text{Tl}_2\text{Ba}_2\text{CaCu}_2\text{O}_{8+\delta}$  at 2.3 GPa based on the tetragonal structure with the space group of  $I4/mmm$ . The middle sticks refer to the peak positions. Inset: Schematic of the crystal structure.

previously [10, 31, 32, 34, 35]. However, it is unclear how pressure would affect the distortion in these compounds. Here we examine the distortion effects on Tl2212 based on these two aspects.

Figure 3 presents the pressure dependence of the lattice parameters along the  $a$  and  $c$  axes, unit-cell volume, and the corresponding axial ratio of  $c/a$ , respectively. Both the lattice parameters and volume do not obviously deviate from the expected equation of state with applied pressure within experimental errors. The compressibility of  $a$  and  $c$ -axes are  $k_a = -\ln(a)/dP = 0.00267 \text{ GPa}^{-1}$ ,  $k_c = -\ln(c)/dP = 0.00356 \text{ GPa}^{-1}$ , respectively, which is well characterized by the Murnaghan equation of state [44, 45]. The similar anisotropic compressibility has also been observed in Tl2212 and  $\text{Tl}_2\text{Ba}_2\text{Ca}_2\text{Cu}_3\text{O}_{10+\delta}$  [46, 47]. The volume compressibility  $k_v = 2k_a + k_c \equiv 1/B_0 = 0.0089 \text{ GPa}^{-1}$ , where  $B_0$  is the bulk modulus at ambient pressure. A bulk modulus of 233 GPa was reported for Tl2212 from early energy dispersive XRD measurements [46]. This value is almost twice of ours for Tl2212. However, our obtained results are comparable to the reported 137 GPa for the trilayer  $\text{Tl}_2\text{Ba}_2\text{Ca}_2\text{Cu}_3\text{O}_{10+\delta}$  [47]. The smaller bulk moduli of 73, 62.5, and 68.56 GPa were also reported for the sister bilayer Bi-based system [48–50]. In analogy with Y124 and Y123 [27, 28], the measured cell volume of Tl2212 does not extend from the expected equation of state in certain more pressure range ( $9 \text{ GPa} < P < 23 \text{ GPa}$ ). The axial ratio of  $c/a$  shows a gradual decrease with increasing pressure till 9 GPa and then exhibits different features with pressure. Our high-quality structural data indicate the increase of the distortion in Tl2212 above 9 GPa.

Note that temperature is also a factor that could change the lattice parameters. Previous study [51] involving pair-distribution function analysis of pulsed neutron-scattering

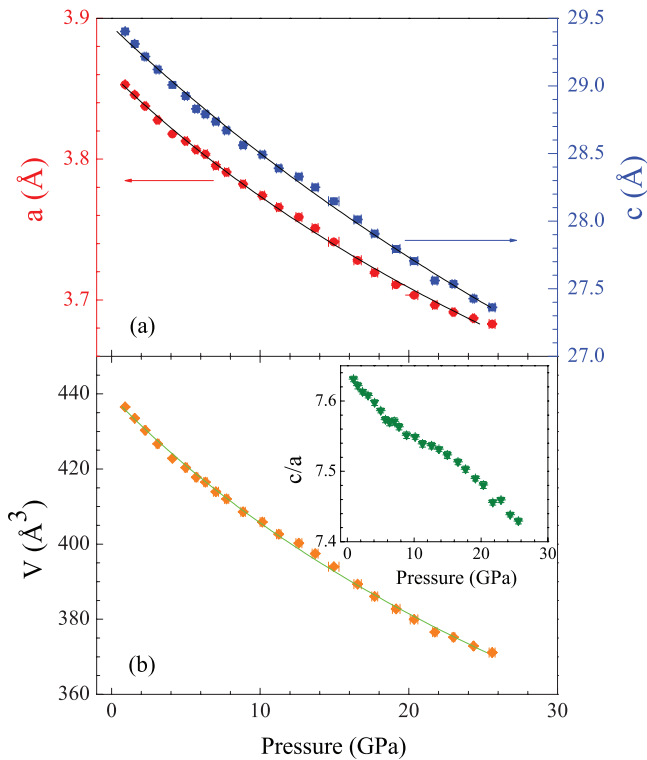


**Figure 3.** The lattice parameters of the  $a$  and  $c$  axes (a) and the unit-cell volume (b) of the nearly optimally doped  $\text{Ti}_2\text{Ba}_2\text{CaCu}_2\text{O}_{8+\delta}$  as a function of pressure up to 25.6 GPa. The solid points are the measured data and the curve is the fitting of the Murnaghan equation of state. Inset: the pressure dependence of the axial ratio of  $c/a$ .

data in  $\text{Ti2212}$  found the O atoms in the Cu–O plane deviate from the average crystallographic structure positions across the superconducting transition. Rietveld analysis of the diffractograms [51] showed no noticeable changes in structural parameters with temperature. This indicates that this local structure change is presumed to have only short-range correlation. The similar short-range ordering of the displacive atomic was observed in  $\text{Ti2212}$  by using the same process [52]. It was shown that Ti and O ions in the Ti–O planes deviate from their ideal high-symmetry positions, creating two possible configurations. However, the ordering remains on the short range and does not alter the average symmetry. The low-temperature refinements from neutron-powder-diffraction data for  $\text{Ti}_2\text{Ba}_2\text{Ca}_2\text{Cu}_3\text{O}_{10+\delta}$  indicated that the symmetry remains tetragonal down to 13 K, indicating no structural change or discontinuity in the cell parameters though  $T_c$  near 125 K [43]. These experimental results indicated no structural phase transition across  $T_c$  for  $\text{Ti2212}$ . Therefore, the structural information obtained at room temperature should shed important insight on the behavior in the superconducting state in  $\text{Ti2212}$ .

### 3.2. Raman scattering

Raman scattering is another powerful experimental method for detecting phase separation/transition and lattice distortions. It can be demonstrated from pressure-induced shift in frequency, mode linewidth, peak emerging or splitting. In the

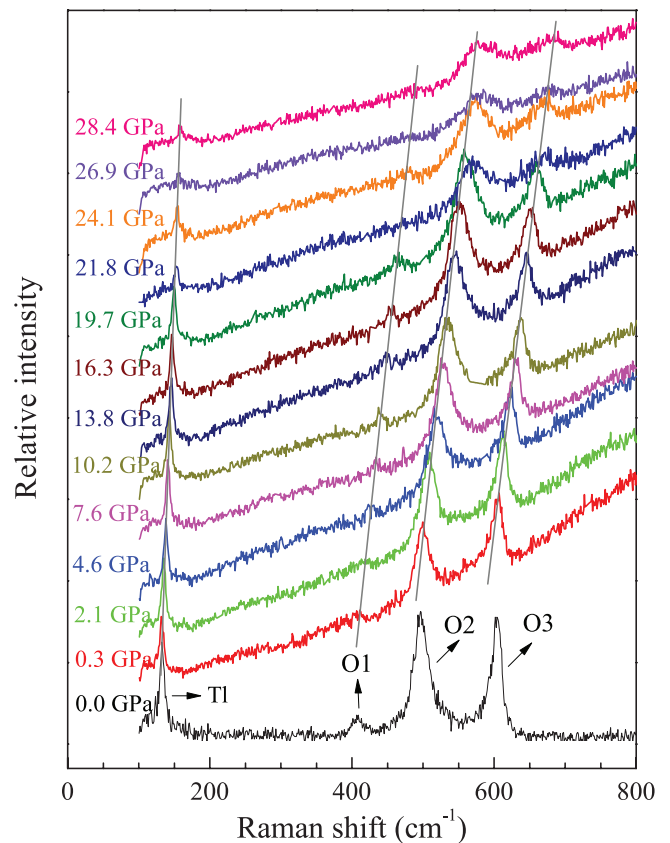


**Figure 4.** Raman spectra of the nearly optimally doped  $\text{Ti}_2\text{Ba}_2\text{CaCu}_2\text{O}_{8+\delta}$  in the frequency range of 100–800  $\text{cm}^{-1}$  at various pressures up to 28.4 GPa. The arrows indicate the  $A_{1g}$  modes of the Ti, O1, O2, and O3 atoms. The gray lines are the guide to eyes.

present study, we have measured the Raman spectra within the region from 100–800  $\text{cm}^{-1}$  as a function of pressure up to 28.4 GPa at room temperature (figure 4). The number of well-resolved modes in the polarized ZZ Raman spectra was six for  $\text{Ti2212}$ . These modes belong to  $A_{1g}$  vibrations as reported in literature [53–59]. The oscillations of Cu and Ba were not studied, due to their small Raman scattering effectiveness [57–59]. The mode at 132  $\text{cm}^{-1}$  can be ascribed to the vibration of Ti. The 409, 497, and 602  $\text{cm}^{-1}$  modes are due to the in-phase angle bending vibrations of oxygen (O1) in the Cu–O planes, oxygen (O2) located in Ba–O planes, and of the oxygen (O3) in the Ti–O planes, respectively. The assignment of these vibrational modes for the studied  $\text{Ti2212}$  is shown in the inset of figure 5(b). There is no indication of peak splitting or merging at high pressures. It should be noted that the bands of vibrational modes O2 and O3 abruptly broaden at pressures above 22 GPa. The vibrational mode of O1 can not be determined due to the weak intensity.

The detailed information for the evolution of frequency shifts and full width at half maximum (FWHM)s of these vibrational modes with pressure is summarized in figure 5. The frequencies of these Raman modes exhibit homogeneous movement before 8.3 GPa, after which the increase of the frequencies exhibit obvious deviations from linear fits. The frequency shifts of the O2 and O3 modes are more sensitive to the applied pressure than that of the Ti mode. The obtained

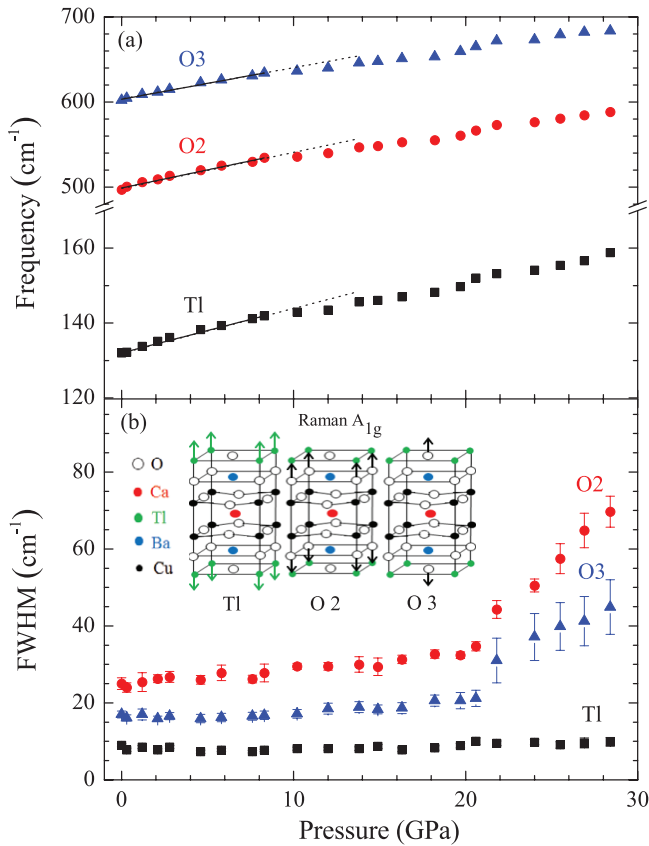


**Figure 5.** Pressure-induced Raman frequency shifts (a) and FWHMs (b) of several selected vibrational modes for the nearly optimally doped  $\text{Ti}_2\text{Ba}_2\text{CaCu}_2\text{O}_{8+\delta}$  single crystal from ambient pressure to 28.4 GPa at room temperature. The lines are the linear fitting results and the dashed lines are extended guiding. Inset: The assignment of the vibrational modes of Tl, O2, and O3 atoms.

behaviors are consistent with other Raman measurements [59], the nonlinear pressure dependence of  $A_{1g}$  modes was reported with applied pressure exceeding 12 GPa. Although the FWHM of the heavy Tl mode still increases systematically with increasing pressure, the two O2 and O3 modes are broadened abruptly above 22 GPa. The deviation of the three vibrational modes from the expected monotonic evolution with pressure indicate the pressure-induced distortion. The sudden change in peak widths of two O2 and O3 modes provides evidence for the enhancement of the distortion of  $\text{Ti}_2\text{212}$  upon heavy compression. This behavior is similar to the observations in other cuprates [60, 61] in which the enhanced distortion occurs at much lower pressures compared to the present compound. Previous studies [62, 63] show there were no anomalies behavior both the frequencies and the linewidths of the  $A_{1g}$  phonon modes from the room temperature to 10 K, further proving its structure shows no obvious temperature dependence as report by pair-distribution function analysis of pulsed neutron-scattering data in  $\text{Ti}_2\text{212}$  [51]. The observed inconsistency for distortion with pressure from XRD and Raman measurements on the samples cleaved from the same crystal of  $\text{Ti}_2\text{212}$  maybe originates from difference of the used pressure transmitting media. Our data does not support the existence of phase transition or phase separation in  $\text{Ti}_2\text{212}$  in the pressure range studied.

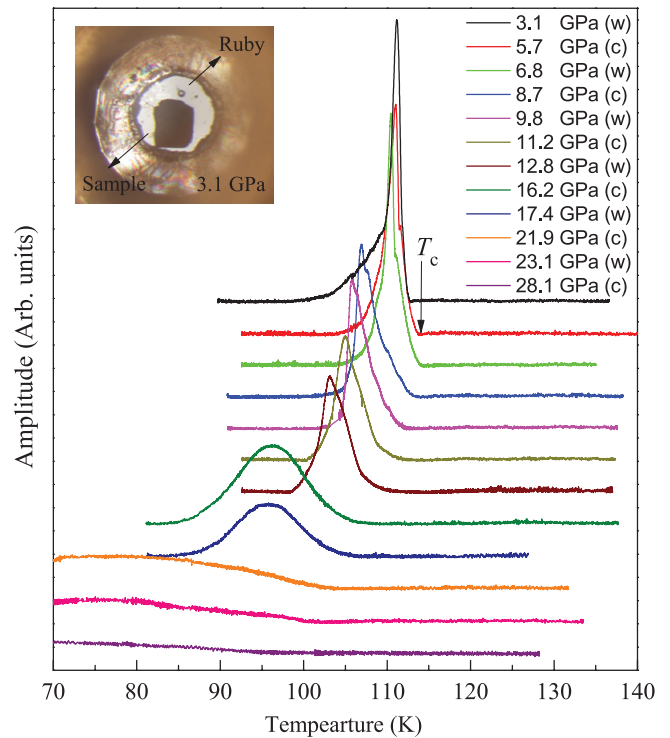


**Figure 6.** Magnetic susceptibility signal for the nearly optimally doped  $\text{Ti}_2\text{Ba}_2\text{CaCu}_2\text{O}_{8+\delta}$  single crystal measured at various pressures up to 28.1 GPa. Inset: The sample and ruby in Daphne 7373 environment in the gasket hole at pressure of 3.1 GPa. W and C stand for warming and cooling processes, respectively.

### 3.3. Superconducting transition

Next we present the results from a systematic high-pressure study on  $T_c$  for  $\text{Ti}_2\text{212}$ . Figure 6 shows the representative temperature scans at different applied pressures. A photograph taken through the diamond windows of a single crystal at 3.1 GPa is shown in the inset. The crystal, together with a small ruby ball, was put in a Daphne 7373 environment in the gasket hole. Large sample was helpful for getting strong amplitude signal. As the pressure transmitting media, Daphne 7373 offers protection for the sample to maintain the bulk feature during measurements at high pressures. For each pressure run, the signal was measured during both cooling and warming cycles at low temperature below 140 K. The pressure was applied and measured at low temperature. Superconducting transition is identified as the temperature where the signal begins to develop on the high-temperature side. The superconducting transition of 109 K was obtained at ambient pressure. It is clear that at the pressure of 6.8 GPa the superconducting transition shifts to higher temperature (114 K), but it returns beyond that pressure. The similar weakening of the amplitude and broadening of the width of the signal upon heavy compression have also been observed in other cuprate superconductors [64, 65].

Figure 7 summarizes the evolution of  $T_c$  of the nearly optimally doped  $\text{Ti}_2\text{212}$  with pressure.  $T_c$  is initially increased with applied pressure and reaches a maximum of 114 K around 6.8 GPa, then decreases at higher pressures. The critical pressure for the occurrence of the maximum  $T_c$  and parabolic-like behavior are similar to those in the sister

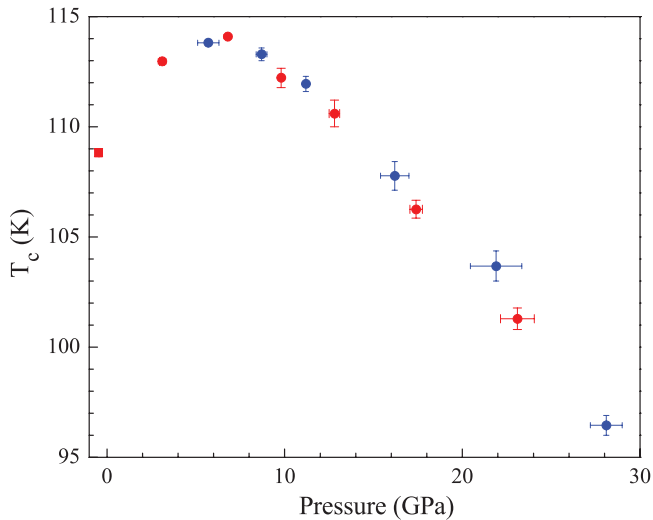


**Figure 7.** Pressure dependence of  $T_c$  for the nearly optimally doped  $\text{Tl}_2\text{Ba}_2\text{CaCu}_2\text{O}_{8+\delta}$  single crystal. The red (blue) solid circles represent the measurements in the warming (cooling) cycle, respectively. Red square represents  $T_c$  at ambient pressure.

optimally doped  $\text{Bi}_2\text{Sr}_2\text{CaCu}_2\text{O}_{8+\delta}$  by using the same measurement technique [64]. Although the amplitude of the single crystal becomes weak with the applied pressure, we still can distinguish the sample signal from the background at pressures up to 28 GPa. The similar parabolic-like behavior with a maximum  $T_c$  around 2.5 GPa (2.0 GPa) has been observed from early experiments by using magnetic susceptibility [66] (resistance [67]) technique. There is only modest increase of  $T_c$  from the initial value to the maximum for both the experiments with the highest pressure less than 4 and 8 GPa, respectively. In the early other measurements [68, 69], the increased  $T_c$  was observed to continue up to the attainable maximum pressure of 6.0 GPa. There is clearly a growing appreciation of the need for  $T_c$  measurements at higher pressures in order to establish the  $T_c$  evolution path. However, the measurements were stopped to 8 GPa for the studied Tl2212 since its discovery [66–71]. The initial pressure derivative of  $T_c$  ( $dT_c/dP$ ) is about  $0.75 \text{ K GPa}^{-1}$  from our measurements. This value is smaller compared to the early measurements at relatively low pressures [66–68, 70, 71]. The difference might be due to the samples with different dopants, sample qualities, and pressure media, or temperatures at which pressure levels were determined [68].

Amongst all the early measurements [66–71], only Moulton *et al* [68] used single crystals and determined pressures at temperatures of about 100 K, those are similar to ours. The others were based on polycrystalline samples [66, 67, 69–71]. For those studies, the  $T_c$  measurements were limited to 8 GPa. Therefore, it is hard to understand the distortion effect on  $T_c$  based on the data obtained at such low pressures with the comparison of the obtained structural and vibrational properties at higher pressures but from different samples [46, 58, 59]. There has been no report or effort of combined measurements on the studied Tl2212 so far. Combining the XRD and Raman spectra, we established the first almost consistent evolution path of the structural and vibrational properties as well as  $T_c$

with pressure of Tl2212 at nearly hydrostatic conditions near 30 GPa by using the samples cleaved from the same single crystal. The nearly optimally doped Tl2212 was found to still hold 89% of its ambient value of  $T_c$  when reducing 15% of the unit-cell volume near 30 GPa. The experimental data based on the same high-quality single crystal but at much higher pressures than before makes the effects of pressure-induced distortion and/or phase separation/transition and pressure effect on superconductivity, and provides an opportunity for the test of any realistic theoretical models over substantial  $T_c$  change.

### 3.4. Intrinsic pressure variables

The obtained parabolic-like  $T_c$  versus  $P$  behavior for the nearly optimally doped Tl2212 with 5 K enhancement of  $T_c$  at a critical pressure about 7 GPa is generic for almost all optimally doped cuprates. This behavior can be explained by many two-component models including charge carrier concentration and another intrinsic variable. For the generally used charge-transfer model, the maximum of  $T_c$  is considered as the other intrinsic variable besides carrier concentration. This simple model worked very well for many cuprates with different dopants [72, 73]. The developed models based on BCS-like gap equations also can be used to reproduce the  $T_c$  variation with pressure for many compounds [74, 75]. The later developments for identifying the pairing interaction strength as the second intrinsic variable has led to many interesting explanations for the  $T_c$  evolution with pressure and its pressure derivatives for compounds with different dopants [64, 76, 77], the uniaxial pressure effect on  $T_c$  [78], the rare-earth ionic size effect on  $T_c$  [77, 79], and even the strain effect on  $T_c$  [80]. This variable has been confirmed by high-pressure NMR measurements [81].

Currently, lattice vibrations and excitations of electronic origin such as spin or electric polarizability fluctuations are believed to be the two most potential candidates of Cooper pairing in the cuprate superconductors. Both were found to have important contributions to the pairing interaction strengths [82, 83]. These indicated that the consideration of pairing interaction strength and carrier concentration maybe sufficient for explaining the observed  $T_c$  behavior in cuprates at high pressures even within the framework of phonon-mediated pairing [84, 85]. The similar two components from the dynamic inhomogeneity-induced pairing model [86] have also been used to explain the experiments [24]. This model includes the pairing scale and the phase ordering scale. The former characterizes pair formation and is proportional to the energy gap. The latter controls the stiffness of the system to phase fluctuations and is determined by the superfluid density. In fact, the superfluid density is approximately proportional to the carrier concentration before the optimal level and the pairing interaction strength should be scaled by the energy gap. Therefore, both the carrier concentration and the pairing interaction strength are two well determined intrinsic pressure variables for cuprate superconductors.

The charge-transfer picture in Tl2212 has been well established experimentally [35]. The pressure-induced reduction of the Hall coefficient has been observed for many cuprates

including the studied Tl2212 [69, 87], indicating the increase of the carrier concentration in the CuO<sub>2</sub> plane. The charge-transfer process can also be monitored by investigating the vibrational frequency of the apical oxygen [88]. We found that the vibration frequency of the apical oxygen (O2) in Tl2212 gets hardening with increasing pressure (see figure 5(a) and also others [58, 59]). The hardening provides the charge transfer from the charge reservoir to the CuO<sub>2</sub> plane, in good agreement with the Hall coefficient measurements [69]. The observations of the increase of both the  $T_c$  and carrier concentration for an overdoped Tl2212 under pressure [69] serve direct evidence for the existence of the other intrinsic pressure variable. Otherwise,  $T_c$  would fall down on the overdoped side due to the increased carrier concentration with pressure if its behavior were solely controlled by the carrier concentration.

Recent experimental efforts shed new light on the nature of the pairing interactions [89, 90]. The typical scale of 2.6 eV was attributed to a fingerprint of ‘Mottness’ in the superconducting state. This energy scale, set by the superexchange interaction, was found to control all  $T_c$ ’s of cuprate superconductors [89]. If the superexchange interaction indeed provides the driving force for superconductivity in cuprates, one can readily learn the pressure effect on the pairing interaction. For almost all cuprate families, the superexchange interaction was clearly found to increase with increasing pressure from Raman scattering measurements [91–93]. The pairing interaction strength as another intrinsic variable is again supported from these experiments.

#### 4. Conclusions

In summary, the evolution of the structure, phonon modes, and superconducting transition temperature with pressure up to near 30 GPa has been obtained for the nearly optimally doped Tl<sub>2</sub>Ba<sub>2</sub>CaCu<sub>2</sub>O<sub>8+δ</sub> samples cleaved from the same piece of single crystal. The structural data from angle-dispersive x-ray diffraction measurements and phonon modes from Raman measurements both confirmed pressure-induced distortion in this compound above 9 GPa. Highly sensitive magnetic susceptibility measurements for the nearly optimally doped Tl<sub>2</sub>Ba<sub>2</sub>CaCu<sub>2</sub>O<sub>8+δ</sub> yielded a generic parabolic-like  $T_c$  behavior upon compression with a maximum around 7 GPa. The transition temperature is initially increase with applied pressure up to 7 GPa, which should be controlled by the competition between the charge carrier density and pairing interaction strength. After passing a maximum, the enhanced distortion contributes to the  $T_c$  reduction. We demonstrated that observed parabolic-like  $T_c$  versus  $P$  behavior for the nearly optimally doped Tl2212 can be explained by the interplay between the intrinsic pressure variables and distortion.

#### Acknowledgments

The XRD measurements were supported by the Cultivation Fund of the Key Scientific and Technical Innovation Project Ministry of Education of China (Project No. 708070). The magnetic susceptibility measurements were supported by the

DOE under Grant No. DE-FG02-02ER45955. The sample design and growth were supported by the Natural Science Foundation of China (Nos. 11120101003 and 11327806). The theoretical analysis was supported by NSAF (No. U1230202). The use of HPCAT, APS was supported by Carnegie Institute of Washington, Carnegie DOE Alliance Center, University of Nevada at Las Vegas, and Lawrence Livermore National Laboratory through funding from DOE-National Nuclear Security Administration, DOE-Basic Energy Sciences, and NSF. APS is supported by DOE-BES, under Contract No. DE-AC02-06CH11357.

#### References

- [1] Tranquada J M, Sternlieb B J, Axe J D, Nakamura Y and Uchida S 1995 *Nature* **375** 561
- [2] Ding H, Yokoya T, Campuzano J C, Takahashi T, Randeria M, Norman M R, Mochiku T, Kadowaki K and Giapintzakis J 1996 *Nature* **382** 51
- [3] He Y *et al* 2012 *Science* **344** 608
- [4] Fujita K *et al* 2014 *Science* **344** 612
- [5] Kohsaka Y *et al* 2007 *Science* **315** 1380
- [6] Wu T, Mayaffre H, Krämer S, Horvatic M, Berthier C, Hardy W N, Liang R-X, Bonn D A and Julien M-H 2011 *Nature* **477** 191
- [7] Ghiringhelli G *et al* 2012 *Science* **337** 821
- [8] Chang J *et al* 2012 *Nat. Phys.* **8** 871
- [9] Lake B *et al* 2002 *Nature* **415** 299
- [10] Torchinsky D H, Mahmood F, Bollinger A T, Bozovic I and Gedik N 2013 *Nat. Mater.* **12** 387
- [11] Attfield J P, Kharlanov A L and Mcallister J A 1998 *Nature* **394** 157
- [12] Mcallister J A and Attfield J P 1999 *Phys. Rev. Lett.* **83** 3289
- [13] Crawford M K, Harlow R L, McCarron E M, Farneth W E, Axe J D, Chou H and Huang Q 1991 *Phys. Rev. B* **44** 7749
- [14] Dabrowski B, Wang Z, Rogacki K, Jorgensen J D, Hitterman R L, Wagner J L, Hunter B A, Radaelli P G and Hinks D G 1996 *Phys. Rev. Lett.* **76** 1348
- [15] Fujita K, Noda T, Kojima K M, Eisaki H and Uchida S 2005 *Phys. Rev. Lett.* **95** 097006
- [16] Eisaki H, Kaneko N, Feng D L, Damascelli A, Mang P K, Shen K M, Shen Z-X and Greven M 2004 *Phys. Rev. B* **69** 064512
- [17] Murai N, Masui T, Ishikado M, Ishida S, Eisaki H, Uchida S and Tajima S 2012 *Phys. Rev. B* **85** 020507
- [18] Gantis A, Calamitoutou M, Palles D, Lampakis D and Liarokapis E 2003 *Phys. Rev. B* **68** 064502
- [19] Calamitoutou M, Gantis A, Margiolaki I, Palles D, Siranidi E and Liarokapis E 2008 *J. Phys.: Condens. Matter* **20** 395224
- [20] Kirkpatrick T R and Belitz D 1992 *Phys. Rev. Lett.* **68** 3232
- [21] Timofeev Y A, Struzhkin V V, Hemley R J, Mao H K and Gregoryanz E A 2002 *Rev. Sci. Instrum.* **73** 371
- [22] Struzhkin V V, Hemley R J, Mao H K and Timofeev Y A 1997 *Nature* **390** 382
- [23] Struzhkin V V, Erements M I, Gan W, Mao H K and Hemley R J 2002 *Science* **298** 1213
- [24] Chen X J, Struzhkin V V, Yu Y, Goncharov A F, Lin C T, Mao H K and Hemley R J 2010 *Nature* **466** 950
- [25] Gao L, Xue Y Y, Chen F, Xiong Q, Meng R L, Ramirez D, Chu C W, Eggert J H and Mao H K 1994 *Phys. Rev. B* **50** 4260
- [26] Drozdov A P, Erements M I, Troyan I A, Ksenofontov V and Shylin S I 2015 *Nature* **525** 73

- [27] Calamiotou M, Gantis A, Siranidi E, Lampakis D, Karpinski J and Liarokapis E 2009 *Phys. Rev. B* **80** 214517
- [28] Calamiotou M, Gantis A, DLampakis D, Siranidi E, Liarokapis E, Margiolaki I and Conder K 2009 *Europhys. Lett.* **85** 26004
- [29] Nakayama A *et al* 2014 *J. Phys. Soc. Japan* **83** 093601
- [30] Souliou S M, Subedi A, Song Y T, Lin C T, Syassen K, Keimer B and Tacon M L 2014 *Phys. Rev. B* **90** 140501
- [31] Koyama Y and Hoshiya H 1989 *Phys. Rev. B* **39** 7336
- [32] Zetterer T, Franz M, Schützmann J, Ose W, Otto H H and Renk K F 1990 *Phys. Rev. B* **41** 9499
- [33] Allen P G, de Leon J M, Conradson S D and Bishop A R 1991 *Phys. Rev. B* **44** 9480
- [34] Koyama y, Nakamura S I, Inoue Y and Ohno T 1992 *Phys. Rev. B* **46** 5757
- [35] Li G G, de Leon J M, Conradson S D, Lovato M V and Subramanian M A 1994 *Phys. Rev. B* **50** 3356
- [36] Ma Y C and Wang N L 2005 *Phys. Rev. B* **72** 104518
- [37] Rivers M, Prakapenka V B, Kubo A, Pullins C, Holl C M and Jacobsen S D 2008 *High Press. Res.* **28** 273
- [38] Hammersley A P, Svensson S O, Hanfland M, Fitch A N and Hausermann D 1996 *High Press. Res.* **14** 235
- [39] Larson A C and Von Dreele R B 1994 GSAS general structure analysis system *Los Alamos National Laboratory Report LAUR 86* (<http://netlib.ccp14.ac.uk/ccp/web-mirrors/pssp/pdf/GSASManual.pdf>)
- [40] Toby B H 2001 *J. Appl. Crystallogr.* **34** 210
- [41] Mao H K, Xu J and Bell P M 1986 *J. Geophys. Res.* **91** 4673
- [42] Subramanian M A, Calabrese J C, Torardi C C, Gopalakrishnan J, Askew T R, Flippen R B, Morrissey K J, Chowdhry U and Sleight A W 1988 *Nature* **332** 420
- [43] Cox D E, Torardi C C, Subramanian M A, Gopalakrishnan J and Sleight A W 1988 *Phys. Rev. B* **38** 6624
- [44] Hyatt N C, Hriljac J A, Miyazaki Y, Gameson I, Edwards P P and Jephcoat A P 2001 *Phys. Rev. B* **65** 014507
- [45] Birch F 1947 *Phys. Rev.* **71** 809
- [46] Webb A W, Qadri S B, Skelton E F, Moulton N E and Vanderah T A 1994 *AIP Conf. Proc.* **309** 691
- [47] Fietz W H, Wassilew C A, Ludwig H A, Obst B, Politis C, Dietrich M R and Wühl H 1990 *High Press. Res.* **4** 423
- [48] Tajima Y, Hikita M, Suzuki M and Hidaka Y 1989 *Physica C* **158** 237
- [49] Olsen J S, Steenstrup S, Gerward L and Sundqvist B 1991 *Phys. Scr.* **44** 211
- [50] Yu J D, Sasaki S, Sugiura H, Huang T, Inaguma Y and Itoh M 1997 *Physica C* **281** 45
- [51] Toby B H, Egami T, Jorgensen J D and Subramanian M A 1990 *Phys. Rev. Lett.* **64** 2414
- [52] Dmowski W, Toby B H and Egami T 1988 *Phys. Rev. Lett.* **61** 2608
- [53] Kulkarni A D, de Wette F W, Prade J, Schröder U and Kress W 1990 *Phys. Rev. B* **41** 6409
- [54] Mori T, Nakaoka K, Onari S and Arai T 1989 *Solid State Commun.* **72** 125
- [55] Mohan S and Sonamuthu K 2002 *Phys. Status Solidi B* **229** 1121–7
- [56] Belosludov V R, Lavrentiev Y M and Syskin S A 1991 *Int. J. Mod. Phys. B* **5** 3109
- [57] Gasparov L V, Kulakovskii V D, Misochko O V, Timofeev V B, kolesnikov N N and Kulakov M P 1989 *J. Exp. Theor. Phys.* **49** 68 ([http://jetpletters.ac.ru/ps/1112/article\\_16832.pdf](http://jetpletters.ac.ru/ps/1112/article_16832.pdf))
- [58] Gasparov L V, Misochko O V, Eremets M I, Lomsadze A V and Struzhkin V V 1990 *Sov. Phys.—JETP* **71** 945 ([www.jetp.ac.ru/cgi-bin/dn/e\\_071\\_05\\_0945.pdf](http://www.jetp.ac.ru/cgi-bin/dn/e_071_05_0945.pdf))
- [59] Timofeev V B, Maksimov A A, Misochko O V and Tartakovskii I I 1989 *Physica C* **162** 1409
- [60] Lampakis D, Palles D, Liarokapis E, Kazakov S M and Karpinski J 2005 *Phys. Rev. B* **72** 014539
- [61] Liarokapis E, Lampakis D, Siranidi E and Calamiotou M 2010 *J. Phys. Chem. Solids* **71** 1084
- [62] Gasparov L V, Kulakovskii V D, Misochko O V, Timofeev V B, Kolesnikov N N and Kulakov M P 1989 *Sov. Phys. JETP* **69** 1196
- [63] Gasparov L V, Kulakovskii V D, Misochko O V, Maksimov A A and Timofeev V B 1989 *Physica C* **160** 147
- [64] Chen X J, Struzhkin V V, Hemley R J, Mao H K and Kendziora C 2004 *Phys. Rev. B* **70** 214502
- [65] Wang S B *et al* 2014 *Phys. Rev. B* **89** 024515
- [66] Allgeier C, Sieburger R, Diederichs J G H, Neumaier H, Reith W, Muller P and Schilling J S 1989 *Physica C* **162** 741
- [67] Mōri N, Takahashi H, Shimakawa Y, Manako T and Kubo Y 1990 *J. Phys. Soc. Japan* **59** 3839
- [68] Moulton N E, Wolf S A, Skelton E F, Liebenberg D H, Vanderah T A, Hermann A M and Duan H M 1991 *Phys. Rev. B* **44** 12632
- [69] Watanabe T *et al* 2003 *J. Low Temp. Phys.* **131** 681
- [70] Schirber J E, Morosin B and Ginley D S 1989 *Physica C* **157** 237
- [71] Han S H, Zhang Y L, Han H and Liu Y 1988 *Physica C* **156** 113
- [72] Chen X J and Jiao Z K 1997 *Phys. Rev. B* **56** 6302
- [73] Chen X J and Gong C D 1999 *Phys. Rev. B* **59** 4513
- [74] Angilella G G N, Pucci R and Siringo F 1996 *Phys. Rev. B* **54** 15471
- [75] De Mello E V L and Acha C 1997 *Phys. Rev. B* **56** 466
- [76] Chen X J, Lin H Q and Gong C D 2000 *Phys. Rev. Lett.* **85** 2180
- [77] Chen X J, Gong C D and Yu Y B 2000 *Phys. Rev. B* **61** 3691
- [78] Chen X J, Lin H Q, Yin W G, Gong C D and Habermeier H-U 2001 *Phys. Rev. B* **64** 212501
- [79] Chen X J and Su H B 2005 *Phys. Rev. B* **71** 094512
- [80] Chen X J, Lin H Q and Gong C D 2000 *Phys. Rev. B* **61** 9782
- [81] Maisuradze A, Shengelaya A, Amato A, Pomjakushina E and Keller H 2011 *Phys. Rev. B* **84** 184523
- [82] Conte S D *et al* 2012 *Science* **335** 1600
- [83] Chia E E M *et al* 2013 *New J. Phys.* **15** 103027
- [84] Chen X J, Struzhkin V V, Wu Z, Lin H Q, Hemley R J and Mao H K 2007 *Proc. Natl Acad. Sci. USA* **104** 3732
- [85] Chen X J, Struzhkin V V, Wu Z, Lin H Q, Hemley R J, Mao H K and Lin H Q 2007 *Phys. Rev. B* **75** 134504
- [86] Emery V J and Kivelson S A 1995 *Nature* **374** 434
- [87] Murayama C, Iye Y, Enomoto T, Mōri N, Yamada Y, Matsumoto T, Kubo Y, Shimakawa Y and Manako T 1991 *Physica C* **183** 277
- [88] Kakihana M, Eriksson S G, Börjesson L, Johansson L G, Ström C and Käll M 1993 *Phys. Rev. B* **47** 5359
- [89] Keren A 2009 *New J. Phys.* **11** 065006
- [90] Mansart B, Lorenzana J, Mann A, Odeh A, Scarongella M, Chergui M and Carbone F 2013 *Proc. Natl Acad. Sci. USA* **110** 4539
- [91] Aronson M C, Dierker S B, Dennis B S, Cheong S-W and Fisk Z 1991 *Phys. Rev. B* **44** 4657
- [92] Maksimov A A and Tartakovskii I I 1994 *J. Supercond.* **7** 439
- [93] Cuk T, Struzhkin V V, Devereaux T P, Goncharov A F, Kendziora C A, Eisaki H, Mao H K and Shen Z-X 2008 *Phys. Rev. Lett.* **100** 217003